

1 **Responses to Referee #1's comments**

2 We are grateful to the reviewers for their valuable and helpful comments on our manuscript “A
3 novel formation mechanism of sulfamic acid and its enhancing effect on methanesulfonic acid-
4 methylamine aerosol particle formation in agriculture-developed and coastal industrial areas”
5 (Manuscript ID: EGUSPHERE-2024-2638). We have revised the manuscript carefully according to
6 reviewers’ comments. The point-to-point responses to the Referee #1’s comments are summarized
7 below:

8 **Referee Comments**

9 The manuscript egusphere-2024-2638, “A novel formation mechanism of $\text{NH}_2\text{SO}_3\text{H}$ and its
10 enhancing effect on methanesulfonic acid-methylamine aerosol particle formation in agriculture-
11 developed and coastal industrial areas”. The work studied the formation of sulfamic acid via HNO_2
12 hydrolysis in the gas phase and at the air-water interface by using theoretical methods. Then, the
13 author investigated the new particle formation for the role of sulfamic acid in $\text{CH}_3\text{SO}_3\text{H}-\text{CH}_3\text{NH}_2$
14 system. The work is very interesting for understanding the chemical processes of sulfamic acid in
15 the atmosphere. However, there are some issues that should be addressed before publication.

16 **Response:** We would like to thank the reviewer for the positive and valuable comments, and we
17 have revised our manuscript accordingly.

18 **Major issues**

19 **Comment 1.**

20 In Line 39, “the concentration of $\text{NH}_2\text{SO}_3\text{H}$ was expected to reach up to $10^8 \text{ molecules} \cdot \text{cm}^{-3}$ ”, the
21 concentration of sulfamic acid was only estimated by theoretical method, not measured by field
22 observations. Therefore, it is required to elucidate this point.

23 **Response:** Thanks for the suggestion of the reviewer. As the suggestion of the reviewer, in Lines
24 38-40 Page 2 of the revised manuscript, the sentence of “**the atmospheric concentration of $\text{NH}_2\text{SO}_3\text{H}$**
25 **was expected to reach up to $10^8 \text{ molecules} \cdot \text{cm}^{-3}$ (Li et al., 2018).**” has been changed as “**the**
26 **atmospheric concentration of SFA estimated by theoretical method of CCSD(T)-F12/cc-pVDZ-**
27 **F12//M06-2X/6-311++G(3df,3pd) (Li et al., 2018)** **was expected to reach up to $10^8 \text{ molecules} \cdot \text{cm}^{-3}$.**”

28 **Comment 2.**

29 Lines 41-42, “the sources of $\text{NH}_2\text{SO}_3\text{H}$ in the atmosphere have been well investigated (Lovejoy and
30 Hanson, 1996; Pszona et al., 2015; Li et al., 2018; Larson and Tao, 2001; Manonmani et al., 2020;
31 Zhang et al., 2022).” In fact, sulfamic acid has been not investigated by field measurements.
32 Therefore, it is not well investigated in the atmosphere.

33 **Response:** Thanks for the suggestion of the reviewer. Indeed, it is true that SFA has not been
34 measured in the field. Therefore, atmospheric sulfamic acid has not been well studied. In Lines 41-
35 43 Page 2 of the revised manuscript, “**So, the sources of $\text{NH}_2\text{SO}_3\text{H}$ in the atmosphere have been**
36 **well investigated (Lovejoy and Hanson, 1996; Pszona et al., 2015; Li et al., 2018; Larson and Tao,**
37 **2001; Manonmani et al., 2020; Zhang et al., 2022).**” has been changed as “**So, the sources of SFA**
38 **in the atmosphere has been focused by several groups (Lovejoy and Hanson, 1996; Pszona et al.,**
39 **2015; Li et al., 2018; Larson and Tao, 2001; Manonmani et al., 2020; Zhang et al., 2022).**”.

40 **Comment 3.**

41 Lines 46-47, “for the hydrolysis of SO_3 assisted by water molecule ($10^{-11}\text{-}10^{-10} \text{ cm}^3 \text{ molecule}^{-1} \text{ s}^{-1}$)
42 (Kim et al., 1998; Hirota et al., 1996; Shi et al., 1994).” Some important references are missing such
43 as J. Am. Chem. Soc. 2023, 145, 19866-19876. and J. Am. Chem. Soc. 1994, 116, 10314–10315.

44 **Response:** Thanks for the suggestion of the reviewer. We apologize for missing some important
45 references. As the suggestion of the reviewer, some important references have been added in Lines
46 46-49 Page 2 of the revised manuscript, which has been organized as “**which was close to the value**
47 **for the hydrolysis of SO_3 assisted by water molecule ($10^{-11}\text{-}10^{-10} \text{ cm}^3 \text{ molecule}^{-1} \text{ s}^{-1}$) (Kim et al.,**
48 **1998; Hirota et al., 1996; Shi et al., 1994; Kolb et al., 1994; Long et al., 2013; Long et al., 2023;**
49 **Ding et al., 2023; Cheng et al., 2023; Wang et al., 2024).**”.

50 **Comment 4.**

51 What is the concentration of HNSO_2 in the atmosphere? This is very necessary for determining the
52 importance of HNSO_2 in the atmosphere.

53 **Response:** Thanks for the suggestion of the reviewer. As the suggestion of the reviewer, we have
54 conducted an extensive review of the relevant literature. However, the concentrations of HNSO_2 in
55 the atmosphere have not been reported. As the absence of the concentration of HNSO_2 , the

56 competitiveness between MSA-assisted HNSO_2 hydrolysis and the NH_3 -assisted ammonolysis of
57 SO_3 (the traditional source of SFA) cannot be further confirmed. The related discussion has been
58 found in Line 236 Page 8 to Line 237 Page 9 of the revised manuscript, which has been organized
59 as “**However, due to the absence of the concentration of HNSO_2 , the competitiveness of these two**
60 **reactions cannot be further confirmed.**” Although the concentration of HNSO_2 has not been reported,
61 it is still important to study HNSO_2 hydrolysis with MSA in the gas phase and at the air-water
62 interface. The detailed importance of HNSO_2 hydrolysis with MSA has been presented as follows.

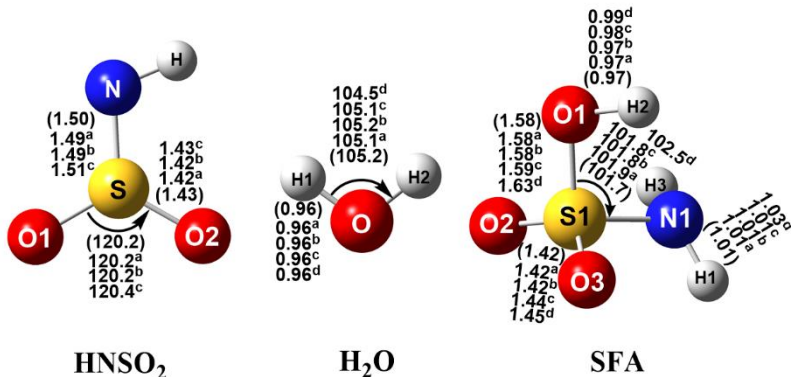
63 In the gas phase, with the significant decrease in atmospheric water molecules with increasing
64 altitude, MSA has a significantly greater catalytic ability than H_2O in accelerating the rate of HNSO_2
65 hydrolysis within 5-15 km. At the air-water interface, two types of reactions, the ions forming
66 mechanism and the proton exchange mechanism to form $\text{NH}_2\text{SO}_3^- \cdots \text{H}_3\text{O}^+$ ion pair were observed
67 on the timescale of picosecond, which is at least two orders of magnitude faster than the
68 corresponding gas-phase reaction. Nobly, considering the overall environment of sulfuric acid
69 emission reduction, the present findings suggest that SFA may play a significant role in NPF and
70 the growth of aerosol particles as *i*) SFA can directly participate in the formation of MSA- CH_3NH_2 -
71 based cluster and enhance the rate of NPF from these clusters by approximately 10^3 times at 278.15
72 K; and *ii*) the NH_2SO_3^- species at the air-water interface can attract gaseous molecules to the aqueous
73 surface, and thus promote particle growth.

74 **Comment 5.**

75 The reliability of the chosen methods should be clarified in the $\text{HNSO}_2 + \text{CH}_3\text{SO}_3\text{H}$ reaction.
76 Although the traditional method CCSD(T)/M06-2X has been widely used for atmospheric reactions,
77 it should be noted that there are quite large uncertainties for estimating barrier height. This should
78 clearly tell the potential readers.

79 **Response:** Thanks for the suggestion of the reviewer. As the suggestion of the reviewer, the
80 reliability of CCSD(T)/aug-cc-pVDZ//M06-2X/6-311+G(2df,2pd)-based calculation method has
81 been verified as follows. Firstly, the geometry and frequency calculation involved in the HNSO_2
82 hydrolysis were verified (Fig. S2) at three different theoretical levels of M06-2X/6-
83 311++G(3df,2pd), M06-2X/6-311++G(3df,3pd) and M06-2X/aug-cc-pVTZ and experimental
84 values. Then, based on the M06-2X/6-311++G(2df,2pd) optimized geometries, the corresponding

85 single point energy calculations (Table S1) were performed at the CCSD(T)-F12/cc-pVDZ-F12,
 86 CCSD(T)-F12/cc-pVTZ-F12, CCSD(T)/CBS and CCSD(T)/aug-cc-pVTZ levels, respectively. The
 87 main revision has been made as follows.



88
 89 **Fig. S2** The optimized geometrical structures for the species involved in the HNSO₂ hydrolysis at
 90 several different levels of theory.

91 a, b and, c respectively represents the values obtained at the M06-2X/6-311++G(3df,2pd), M062X/6-311++G(3df,3pd)
 92 and M06-2X/aug-cc-pVTZ level of theory, ^d represents the experimental values (The values in parentheses were
 93 obtained at the M06-2X/6-311++G(2df,2pd) level of theory; bond length is in angstrom and angle is in degree.).

94 (a) The geometric parameters of the reactants of HNSO₂, H₂O and NH₂SO₃H (SFA) have been
 95 displayed in Fig. S2. As seen in Fig. S2, the mean absolute deviation of calculated bond distances
 96 and bond angles between the M06-2X/6-311++G(2df,2pd) level and the experimental reports were
 97 0.02 Å and 0.57°, respectively. This reveals that the calculated bond distances and bond angles at
 98 the M06-2X/6-311++G(2df,2pd) level agree well with the available experimental values (From the
 99 pubchem database, <https://pubchem.ncbi.nlm.nih.gov/#opennewwindow>). In addition, we have re-
 100 optimized all equilibrium structures of HNSO₂, H₂O and NH₂SO₃H at three different theoretical
 101 levels of M06-2X/6-311++G(3df,2pd), M062X/6-311++G(3df,3pd) and M06-2X/aug-cc-pVTZ
 102 levels. For the calculated geometrical parameters of these species, the mean absolute deviation of
 103 calculated bond distances and bond angles between the M06-2X/6-311++G(2df,2pd) level and the
 104 other levels were within 0.02 Å and 0.2°, respectively. Therefore, due to its efficiency, the M06-
 105 2X/6-311++G(2df,2pd) was adopted to optimize the geometries of all stationary points involved in
 106 the HNSO₂ hydrolysis. Based on this, in Lines 121 to 124 Page 5 of the revised manuscript, the
 107 sentence of “It is noted that the calculated bond distances and bond angles at the M06-2X/6-
 108 311++G(2df,2pd) level (Fig. S2) agree well with the available values (Fig. S2) from the experiment
 109 and three different theoretical levels of M06-2X/6-311++G(3df,2pd), M062X/6-311++G(3df,3pd)
 110 and M06-2X/aug-cc-pVTZ levels.” has been added.

111 **Table S1** The Energy barriers (ΔE) and unsigned error (UE) (kcal·mol⁻¹) for the HNSO₂ hydrolysis
 112 at different theoretical the potential energy profile (ΔG) correction

Methods	ΔE^a	ΔE^b	ΔE^c	UE
CCSD(T)/CBS//M06-2X/ 6-311++G(2df,2pd)	3.4	29.7	-23.0	0.00
CCSD(T)-F12/cc-pVDZ-F12//M06-2X/ 6-311++G(2df,2pd)	3.6	30.6	-22.0	0.71

113 ^{a, b and c} respectively denote the species of pre-reactive complexes, transition states and products involved in the
 114 HNSO₂ hydrolysis.

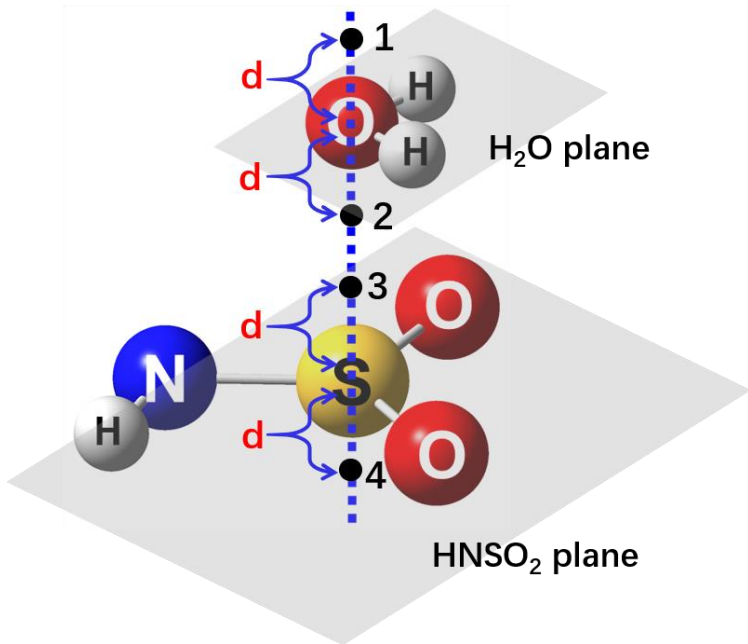
115 (b) To further confirm the reliability of the CCSD(T)-F12/cc-pVDZ-F12//M06-2X/6-
 116 311++G(2df,2pd) level of theory, single-point energy calculations for the HNSO₂ hydrolysis in the
 117 gas phase have been performed at two different levels of CCSD(T)/CBS and CCSD(T)-F12/cc-
 118 pVDZ-F12 based on the optimized geometries at the M06-2X/6-311++G(2df,2pd) level. Notably,
 119 the complete basis set (CBS) obtained by basis set extrapolation is used as the reference basis set.
 120 As presented in Table S1, compared with unsigned error calculated at the CCSD(T)/CBS//M06-
 121 2X/6-311++G(2df,2pd) level, unsigned errors calculated at CCSD(T)-F12/cc-pVDZ-F12//M06-
 122 2X/6-311++G(2df,2pd) was 0.71 kcal·mol⁻¹. This suggests that the relative energies obtained at the
 123 CCSD(T)/aug-cc-pVDZ//M06-2X/6-311+G(2df,2pd) level was reasonable. Considering the
 124 computational accuracy and cost, the CCSD(T)/aug-cc-pVDZ//M06-2X/6-311+G(2df,2pd) method
 125 was chosen to calculate the single point energies of all the species involved in the HNSO₂ hydrolysis.
 126 Thus, in Lines 130 to 133 Page 5 of the revised manuscript, the sentence of “**The CCSD(T)/aug-cc-**
 127 **pVDZ method was chosen to calculate the relative energies as the fact that, compared with unsigned**
 128 **error (Table S1) calculated at the CCSD(T)/CBS//M06-2X/6-311++G(2df,2pd) level, unsigned**
 129 **errors calculated at CCSD(T)-F12/cc-pVDZ-F12//M06-2X/6-311++G(2df,2pd) was 0.71 kcal·mol⁻**
 130 **1.**” has been added.

131 **Comment 6.**

132 In kinetics calculations, it is unclear. There are lots of issues that must be addressed. Provide the
 133 details of VRC calculations. For example, how to set pivot points and what is the electronic structure
 134 method for VRC-TST calculations? The author should provide the input files for VRC-TST and
 135 MESMER calculations in Supporting information to help the potential readers to understand the
 136 computational details.

137 **Response:** Thanks for the suggestion of the reviewer. The pivot point setting method and the
138 electronic structure method for VRC-TST calculation are provided in detail (shown in Part S1 in the
139 Supplement). Meanwhile, the input files for VRC-TST and MESMER calculations have been
140 provided in Supporting information. The main revision has been made as follows.

141 (a) Herein, we describe the implementation details of the VRC-TST calculation in Part S1
142 in the Supplement. Specifically, there are two assumptions in VRC-VTST calculation: (1) the
143 contribution of the vibrational modes of reactants to the partition function is canceled by the
144 corresponding contribution of transition states to the partition function; (2) the internal geometries
145 of reactants are fixed along the reaction coordinate. The reaction coordinate in VRC-VTST is
146 different from that in RP-VTST and determined by the pivot points of each reactant fragment. For
147 the HNSO_2 hydrolysis reaction, the pivot points of HNSO_2 (points 1 and 2) are located at a distance
148 $\pm d$ along its S axis. Meanwhile, the pivots of H_2O (points 3 and 4) are located at a distance $\pm d$
149 perpendicular to H_2O molecule lane. As shown in Fig. S6, the Multiwfn package combined with the
150 VMD software is adopted to visualize the reaction system and help determine the location of pivot
151 points. The reaction coordinate value (s) is defined as the minimum of the distance (r_{ij}) between the
152 pivot point i (=1 or 2) and pivot point j (=3 or 4), where i and j represent the pivot points of HNSO_2
153 and H_2O molecules, respectively. Hence, each of the four dividing surfaces is obtained by
154 symmetrically placing two pivot points of each radical fragment (1-3, 1-4, 2-3, and 2-4). For
155 example, if the reaction coordinate s is equal to r_{23} , one of the four dividing surfaces (2-3), is
156 determined by the locations of pivot points 2, 3 and the reaction coordinate s . There are total four
157 pair of pivot points, the other three dividing surfaces (1-3, 1-4, 2-4) are defined by their
158 corresponding pivot points and reaction coordinates s . Note that the locations of pivot points are
159 critical to the rate constant calculation. Considering the difference between HNSO_2 and H_2O
160 molecules, the distance s between pivot points varies from 2.5 to 6 Å for HNSO_2 and H_2O in each
161 case with a 0.5 Å grid increment. So, in Lines 139 to 141 Page 5 of the revised manuscript, the
162 sentence of the “Meanwhile, two pivot points (Bao et al., 2016; Long et al., 2021; Georgievskii and
163 Klippenstein, 2003; Meana-Pañeda et al., 2024) were selected to calculate the high-pressure limiting
164 rate for the HNSO_2 hydrolysis (shown in Part S1 in the Supplement).” has been added. Also, the
165 computational details of VRC-VTST calculations have been added in Line 159 Page S15 to 180 Page
166 S16 of the revised Supplement.



167

168

Fig. S6 The placements of the pivot points for the HNSO_2 hydrolysis

169

170

171

172

173

(b) The electronic structure method for VRC-TST calculations is based on Gaussian 09 program using the M06-2X/6-311++G(2df,2pd). So, in Lines 137-139 Page 5 of the revised manuscript, the sentence of the “**It's worth noting that the electronic structure method for VRC-TST calculations is based on Gaussian 09 program using the M06-2X/6-311++G(2df,2pd).**” has been added.

174

(c) The input files for VRC-TST and MESMER calculations have been provided in Supplement.

175

Comment 7.

176

177

178

179

180

According to the authors' previous research (*Phys. Chem. Chem. Phys.*, 2022, 24, 4966-4977), the reaction of HNSO_2 with $n\text{H}_2\text{O}$ also has a sufficiently low free energy barrier, which implies that HNSO_2 can undergo hydrolysis or decomposition directly at the gas-liquid interface or in the bulk phase. This seems to contradict the explanation on line 228 (page 8), given that the concentration of water is sufficiently high.

181

182

183

184

185

186

Response: Thanks for the suggestion of the reviewer. According to the previous work (*Phys. Chem. Chem. Phys.*, 2022, 24, 4966-4977), the hydrolysis of HNSO_2 assisted by H_2O , $(\text{H}_2\text{O})_2$ and $(\text{H}_2\text{O})_3$ involved a loop structure mechanism. These reactions were known to occur via the initial formation of ring hydrogen bonding complex $\text{HNSO}_2\cdots(\text{H}_2\text{O})_n$ ($n = 1-3$) with the calculated relative free energy of 0.2-3.6 $\text{kcal}\cdot\text{mol}^{-1}$ followed by their rearrangement to form $\text{NH}_2\text{SO}_3\text{H}$. As the higher entropy effect, hydrogen bonding complex $\text{HNSO}_2\cdots(\text{H}_2\text{O})_n$ ($n = 1-3$) were formed hardly under

187 actual atmospheric conditions, and thus the loop structure mechanism for the hydrolysis of HNSO_2
188 assisted by H_2O , $(\text{H}_2\text{O})_2$ and $(\text{H}_2\text{O})_3$ is not easy to occur in the gas phase. This is similar with
189 $\text{CH}_3\text{SO}_3\text{H}$ -assisted gaseous hydrolysis of HNSO_2 which does not occur within the 100 ps.

190 At the air-water interface, the HNSO_2 molecule is stable and does not dissociate within 10 ps,
191 where the loop structure of hydrogen bonding complex $\text{HNSO}_2\cdots(\text{H}_2\text{O})_n$ ($n = 1-3$) has not been
192 observed. This is proved by the BOMD simulation illustrated in Fig. S8 where the hydrated form of
193 HNSO_2 was not conducive to HNSO_2 hydrolysis at the air-water interface. So, even if the
194 concentration of water molecules at the air-water interface is sufficiently high, the probability that
195 HNSO_2 can be hydrolyzed or decomposed either directly at the air-water interface or in the bulk
196 phase is small. This is agreed with the simulation results. Based on this analysis above, in Lines
197 272-274 Page 10 of the revised manuscript, the sentence of the “**Meanwhile, although HNSO_2**
198 **remains stable at the air-water interface (seen in Fig. S8) and does not dissociate within 10 ps, the**
199 **hydrated form of HNSO_2 illustrated in Fig. S8 was not conducive to HNSO_2 hydrolysis at the air-**
200 **water interface.**” has been added to prove that the hydrated form of HNSO_2 was not conducive to
201 HNSO_2 hydrolysis at the air-water interface.

202 **Comment 8.**

203 Why did the authors not consider a third access channel in the gas phase, that is, the reaction pathway
204 of $\text{HNSO}_2\cdots\text{CH}_3\text{SO}_3\text{H} + \text{H}_2\text{O}$? Considering the reactions at the gas-liquid interface, it seems more
205 plausible that $\text{HNSO}_2\cdots\text{CH}_3\text{SO}_3\text{H}$ would first form a complex before reacting with water molecules.
206 Considering the reactions at the gas-liquid interface, it seems more plausible that $\text{HNSO}_2\cdots$
207 $\text{CH}_3\text{SO}_3\text{H}$ would first form a complex before reacting with water molecules.

208 **Response:** Thanks for the suggestion of the reviewer. Indeed, the reaction pathway of $\text{HNSO}_2\cdots$
209 $\text{MSA} + \text{H}_2\text{O}$ is feasible. However, the concentration of water molecules in the atmosphere is about
210 10^{18} molecules $\cdot\text{cm}^{-3}$, which is much higher than those of HNSO_2 and MSA ($10^5\text{-}10^9$ molecules $\cdot\text{cm}^{-3}$). Considering the harsh conditions for the initial formation of dimers between HNSO_2 and MSA
212 (i.e., HNSO_2 and MSA are sufficiently concentrated in the atmosphere.), we predict that the primary
213 preliminary dimers will continue to be dominated by $\text{HNSO}_2\cdots\text{H}_2\text{O}$ and $\text{MSA}\cdots\text{H}_2\text{O}$ complexes.
214 So, in Line 203 Page 7 to Line 207 Page 8 of the revised manuscript, the sentence of the “**As the**
215 **concentration of water molecule (10^{18} molecules $\cdot\text{cm}^{-3}$ (Anglada et al., 2013)) in the atmosphere is**

216 much higher than those of HNSO_2 and MSA ($10^5\text{-}10^9$ molecules· cm^{-3} (Shen et al., 2020)), the
217 reaction pathway of $\text{HNSO}_2\cdots\text{MSA} + \text{H}_2\text{O}$ is hard to occur in actual atmospheric conditions. So,
218 Channel MSA proceeds through the initial formation of dimers ($\text{HNSO}_2\cdots\text{H}_2\text{O}$ and $\text{MSA}\cdots\text{H}_2\text{O}$)
219 via collisions between HNSO_2 (or MSA) and $\text{H}_2\text{O}.$ ” has been added.

220 **Comment 9.**

221 In Section 3.3, the authors examined the impact of MSA-MA-SFA clusters on nucleation.
222 Interestingly, DMA, which has a stronger nucleation capability, and NH_3 , which has a higher
223 concentration, were excluded. I would like the authors to provide some appropriate justifications
224 for this.

225 **Response:** Thanks for the suggestion of the reviewer. Previous studies have demonstrated that
226 MSA-driven new particle formation (NPF) has attracted growing attention, as MSA significantly
227 contributes to NPF in scenarios with only natural sources of SO_2 were present. Currently,
228 atmospheric bases, including methylamine (MA), monoethanolamide, and dimethylamine (DMA),
229 have a key role in MSA-driven aerosol particle generation and growth, where MA exhibits the
230 strongest enhancing capability (*Environ. Sci. Technol.*, 2017, 51, 243-252; *J. Phys. Chem. B*, 2016,
231 120, 1526-1536; *Environ. Sci. Technol.*, 53, 14387-14397, 2019; *Atmos. Environ.*, 2023, 311,
232 120001). So, we choose MA over DMA and NH_3 . This choice is similar to that previously reported
233 in the relevant references (*Atmos. Chem. Phys.*, 22, 2639-2650; 2022 *Atmos. Environ.*, 2023, 311,
234 120001). Based on this analysis above, in Lines 94-96 Page 4 of the revised manuscript, the sentence
235 of the “Initially, the binary nucleation of MSA with inorganic ammonia and organic amines in the
236 atmosphere has been reported, where MA exhibits the strongest enhancing capability (Chen et al.,
237 2016; Chen and Finlayson-Pitts, 2017; Shen et al., 2019; Hu et al., 2023).” has been reorganized to
238 prove that the MSA-MA system was chosen over MSA-DMA.

239 **Comment 10.**

240 Since the ammonolysis of SO_3 is the primary pathway for SFA formation, the authors could have
241 compared it with the current pathway, which would be necessary for accurately assessing the
242 atmospheric significance of the current reaction.

243 **Response:** Thanks for the suggestion of the reviewer. As the suggestion of reviewer, we compared
244 the NH₃-assisted ammonolysis of SO₃ with the MSA-assisted HNSO₂ hydrolysis. In Line 233 Page
245 8 to Line 237 Page 9 of the revised manuscript, “**Besides, MSA-assisted HNSO₂ hydrolysis is**
246 **reduced by 4.9 kcal·mol⁻¹ in energy barrier than the NH₃-assisted ammonolysis of SO₃ with its rate**
247 **constant at 298 K (2.85 × 10⁻¹¹ cm³·molecule⁻¹·s⁻¹) close to the value of ammonolysis of SO₃ with**
248 **NH₃ (4.35 × 10⁻¹⁰ cm³·molecule⁻¹·s⁻¹) (Li et al., 2018).** However, due to the absence of the
249 concentration of HNSO₂, the competitiveness of these two reactions cannot be further confirmed.”
250 has been added.

251 **Comment 11.**

252 In Fig. 6b and Fig. 7b, it is necessary for the authors to carefully examine whether the significant
253 abrupt changes caused by the concentrations of SFA and MA are reasonable.

254 **Response:** Thanks for the suggestion of the reviewer. It is noted that in Fig. 6(b), due to the
255 competitive relationship between MSA and SFA, at low concentrations of SFA, the binding capacity
256 of MSA with MA is stronger than that of SFA with MA, resulting in only a small amount of SFA
257 participating in cluster formation. However, as the concentration of SFA increases, the number of
258 (MSA)_x·(MA)_y·(SFA)_z (where $y \leq x + z \leq 3$) ternary clusters increases, leading to the formation of
259 more hydrogen bonds and a significant increase in R_{SFA} . Similarly, in Fig. 7(b), at a certain
260 concentration of SFA and MA, as the concentration of MSA increases, the hydrogen bonds between
261 SFA and MA are disrupted, leading to more binding of MA and MSA rather than SFA, resulting in
262 a sharp decrease in R_{SFA} . In Lines 364-369 Page 12 of the revised manuscript, “**It is noted that in**
263 **Fig. 6(b), due to the competitive relationship between MSA and SFA, at low concentrations of SFA,**
264 **the binding capacity of MSA with MA is stronger than that of SFA with MA, resulting in only a**
265 **small amount of SFA participating in cluster formation. However, as the concentration of SFA**
266 **increases, the number of (MSA)_x·(MA)_y·(SFA)_z (where $y \leq x + z \leq 3$) ternary clusters increase,**
267 **leading to the formation of more hydrogen bonds and a significant increase in R_{SFA} .**” has been added.

268 **Comment 12.**

269 In the introduction, the authors mention that the pK_a may affect the transfer of protons, thereby
270 affecting the catalytic ability. Whether similar trends will also directly affect the nucleation

271 capability should be considered, such as in the cases of MSA-MA-SFA, MSA-MA-SA, and SA/FA-
272 MA-SFA.

273 **Response:** Thanks for the suggestion of the reviewer. We apologize for the misunderstanding about
274 pK_a in Lines 63-65 Pages 2-3. Indeed, our aim is to illustrate the importance of MSA as a catalyst
275 from pK_a perspective. In order not to create ambiguity, as for the discussions of pK_a , the sentence
276 of the “**It was noted that as the acidity of CH_3SO_3H ($pK_a = -1.92$) was significantly stronger than**
277 **that of water ($pK_a = 15.0$) and formic acid ($pK_a = 3.74$), it may be predicted that the proton transfer**
278 **reaction for the hydrolysis of $HNSO_2$ with CH_3SO_3H was much easier than those with water and**
279 **formic acid. It was also noted that although CH_3SO_3H was less acidic than H_2SO_4 ($pK_a = -3.00$),**
280 **with the global reduction in the concentration of H_2SO_4 resulting from SO_2 emission restrictions,**
281 **the contribution of CH_3SO_3H to aerosol nucleation has received the widespread attention of**
282 **scientists.**” had been deleted. Meanwhile, the importance of MSA as a catalyst in $HNSO_2$ hydrolysis
283 has been organized as “**It was noted that, with the global reduction in the concentration of H_2SO_4**
284 **resulting from SO_2 emission restrictions, the contribution of MSA to aerosol nucleation has received**
285 **the widespread attention of scientists.**” in Lines 63-66 Page 3 of the revised manuscript.

286

287 **Responses to Referee #2's comments**

288 We are grateful to the reviewers for their valuable and helpful comments on our manuscript “A
289 novel formation mechanism of sulfamic acid and its enhancing effect on methanesulfonic acid-
290 methylamine aerosol particle formation in agriculture-developed and coastal industrial areas”
291 (Manuscript ID: EGUSPHERE-2024-2638). We have revised the manuscript carefully according to
292 reviewers’ comments. The point-to-point responses to the Referee #2’s comments are summarized
293 below:

294 **Referee Comments**

295 Wang et al. present a novel formation mechanism of sulfamic acid ($\text{NH}_2\text{SO}_3\text{H}$) and its
296 enhancement effect in methanesulfonic acid-methylamine (MSA-MA) aerosol particle formation.
297 The study centers on the production, consumption, and potential pollution impacts of sulfamic acid
298 over agriculture-intensive and coastal industrial regions. The most part of this manuscript is well
299 written and of broad interest to the readership of *Atmospheric Chemistry and Physics*. I recommend
300 publication in *Atmospheric Chemistry and Physics* after the following comments have been
301 addressed.

302 **Response:** We would like to thank the reviewer for the positive and valuable comments, and we
303 have revised our manuscript accordingly.

304 **Major issues**

305 **Comment 1.**

306 Pages 2-3 lines 57-62: “As the direct hydrolysis of HNSO_2 with a high energy barrier takes place
307 hardly in the gas phase, the addition of a second water molecule, formic acid and sulfuric acid
308 (H_2SO_4 , SA) have been proved to promote the product of $\text{NH}_2\text{SO}_3\text{H}$ through the hydrolysis of
309 HNSO_2 . However, to the best of our knowledge, the gaseous hydrolysis of HNSO_2 with $\text{CH}_3\text{SO}_3\text{H}$
310 has not yet been investigated”

311 The necessity for studying the gaseous hydrolysis of HNSO_2 with $\text{CH}_3\text{SO}_3\text{H}$ is not sufficiently
312 clarified. Is there any research or evidence indicating that the reaction processes you introduced
313 earlier are insufficient to explain the source of sulfamic acid? If so, please provide additional
314 information.

315 **Response:** Thanks for the suggestion of the reviewer. We apologize for not explicitly studying the
316 necessity for studying the gaseous hydrolysis of HNSO_2 with MSA. According to the reviewer's
317 suggestion, the main revision of the necessity for studying the gaseous hydrolysis of HNSO_2 with
318 MSA has been made as follows.

319 (a) In fact, the gaseous hydrolysis of HNSO_2 with MSA was very important at two points.
320 Firstly, with the global reduction in the concentration of H_2SO_4 resulting from SO_2 emission
321 restrictions, the contribution of MSA to aerosol nucleation has received the widespread attention of
322 scientists. As a major inorganic acidic air pollutant (*Chemosphere*, 2020, 244, 125538-125547),
323 the concentration of MSA in the atmosphere was noted to be notably high across various regions,
324 spanning from coastal to continental, with levels found to be between 10% and 250% of those
325 measured for SA (*Environ. Sci. Technol.*, 2019 53, 14387-14397; *Environ. Sci. Technol.*, 2020,
326 54, 13498-13508; *J. Phys. Chem. A*, 2014 118, 5316-5322; *Atmos. Environ.*, 2023, 311, 120001).
327 Based on the analysis above, the importance of MSA has been reorganized as “**It was noted that,**
328 **with the global reduction in the concentration of H_2SO_4 resulting from SO_2 emission restrictions,**
329 **the contribution of MSA to aerosol nucleation has received the widespread attention of scientists.**
330 As a major inorganic acidic air pollutant (Chen et al., 2020), the concentration of MSA in the
331 atmosphere was noted to be notably high across various regions, spanning from coastal to
332 continental, with levels found to be between 10% and 250% of those measured for SA (Shen et al.,
333 2019; Dawson et al., 2012; Bork et al., 2014; Shen et al., 2020; Berresheim et al., 2002; Hu et al.,
334 2023).” in the Lines 63-70 Page 3 of the revised manuscript. Secondly, the gaseous hydrolysis of
335 HNSO_2 with MSA has not yet been investigated, which will confine the understanding for the source
336 of SFA in regions with significant pollution and high levels of MSA. So, the necessity for studying
337 the gaseous hydrolysis of HNSO_2 with MSA has been added as “**However, to the best of our**
338 **knowledge, the gaseous hydrolysis of HNSO_2 with MSA has not yet been investigated, which will**
339 **confine the understanding for the source of SFA in regions with significant pollution and high levels**
340 **of MSA.**” in Lines 70-72 Page 3 of the revised manuscript.

341 (b) The traditional view is that the source of sulfamic acid primarily originates from the
342 ammonolysis of SO_3 in the troposphere, which has been widely reported by many groups (*J. Am.*
343 *Chem. Soc.*, 2018, 140, 11020-11028; *J. Phys. Chem. A*, 2019, 123, 14, 3131-3141; *J. Mass*
344 *Spectrom.*, 50, 127-135, 2015). In addition to the traditional source of sulfamic acid, the hydrolysis

345 of HNSO_2 has garnered increasing attention as a potential new source of sulfamic acid.
346 Consequently, the hydrolysis of HNSO_2 with MSA has been studied in this paper. To date, the
347 atmospheric concentration of sulfamic acid has only been estimated in the $\text{SO}_3\text{-NH}_3$ system by Li
348 et al (*J. Am. Chem. Soc.*, 2018, 140, 11020-11028) using the theoretical method, no field
349 observations of atmospheric sulfamic acid concentrations have been reported. So, the contribution
350 of the HNSO_2 hydrolysis with MSA to atmospheric sulfamic acid sources remains uncertain.
351 However, “A novel formation mechanism of sulfamic acid and its enhancing effect on
352 methanesulfonic acid-methylamine aerosol particle formation in agriculture-developed and coastal
353 industrial areas” not only elucidates a novel mechanism underlying the hydrolysis of HNSO_2 with
354 MSA, but also highlight the potential contribution of sulfamic acid on aerosol particle growth and
355 new particle formation.

356 **Comment 2.**

357 Page 6 lines 155-156: “The ACDC model was utilized to simulate the $(\text{SFA})_x(\text{MSA})_y(\text{MA})_z$ ($0 \leq$
358 $z \leq x + y \leq 3$) cluster formation rates and explore the potential mechanisms”. The structural
359 stability of clusters directly impacts the nucleation ability of a multi-components system. How was
360 the most stable structure of $(\text{SFA})_x(\text{MSA})_y(\text{MA})_z$ ($0 \leq z \leq x + y \leq 3$) clusters used in this
361 paper obtained?

362 **Response:** Thanks for the suggestion of the reviewer. The most stable structure of
363 $(\text{SFA})_x(\text{MSA})_y(\text{MA})_z$ ($0 \leq z \leq x + y \leq 3$) clusters were searched with ABCluster software
364 (Zhang and Dolg, 2015). In Lines 169-173 Page 6 of the revised manuscript, the sentence of “**The**
365 **ACDC model was utilized to simulate the $(\text{SFA})_x(\text{MSA})_y(\text{MA})_z$ ($0 \leq z \leq x + y \leq 3$) cluster**
366 **formation rates and explore the potential mechanisms.**” has been reorganized as “**The ACDC model**
367 **(McGrath et al., 2012; Hu et al., 2023; Zhao et al., 2020; Zhang et al., 2024; Tsona Tchinda et**
368 **al., 2022; Liu et al., 2020) was utilized to simulate the $(\text{MSA})_x(\text{MA})_y(\text{SFA})_z$ ($0 \leq y \leq x + z \leq 3$)**
369 **cluster formation rates and explore the potential mechanisms, where the most stable structure of**
370 **$(\text{SFA})_x(\text{MSA})_y(\text{MA})_z$ ($0 \leq z \leq x + y \leq 3$) clusters were searched with ABCluster software**
371 **(Zhang and Dolg, 2015) (The details in Part S2 of the Supplement).**”. In Part S2 of the Supplement,
372 the specific steps of configurational sampling have been added as “**A multistep global minimum**
373 **sampling scheme, which has previously been applied to study the atmospheric cluster formation,**

374 was employed to search for the global minima of the $(SFA)_x(MSA)_y(MA)_z$ ($0 \leq z \leq x + y$
375 ≤ 3) clusters. To locate the global minimum energy structure, the artificial bee colony
376 algorithm was systematically employed by the ABCluster program to generate $n \times 1000$ ($1 < n$
377 ≤ 4) initial random configurations for each cluster, and then, PM6 semi-empirical method was
378 used to further pre-optimize the produced configurations above. Second, up to 100 structures
379 with relatively lower energies were selected from the $n \times 1000$ structures (where $1 < n \leq 4$),
380 and a M06-2X/6-31+G(d,p) level of theory was applied for subsequent optimization. Finally,
381 further geometry optimization and frequency calculations at the M06-2X/6-311++G(2df,2pd)
382 level of theory were performed to optimize the 10 best of 100 optimized configurations, and
383 then the global minimum structure with the lowest energy was obtained. Subsequently, the
384 M06-2X function combined with the 6-311++G(2df,2pd) basis set was chosen as it has been
385 proven to be accurate in estimating the thermodynamic properties of atmospheric clusters, such
386 as organic acid-SA-amine clusters, amide-SA clusters or amino acid-SA clusters. In this study,
387 all the density functional theory (DFT) calculations were implemented in the Gaussian 09
388 program.”.

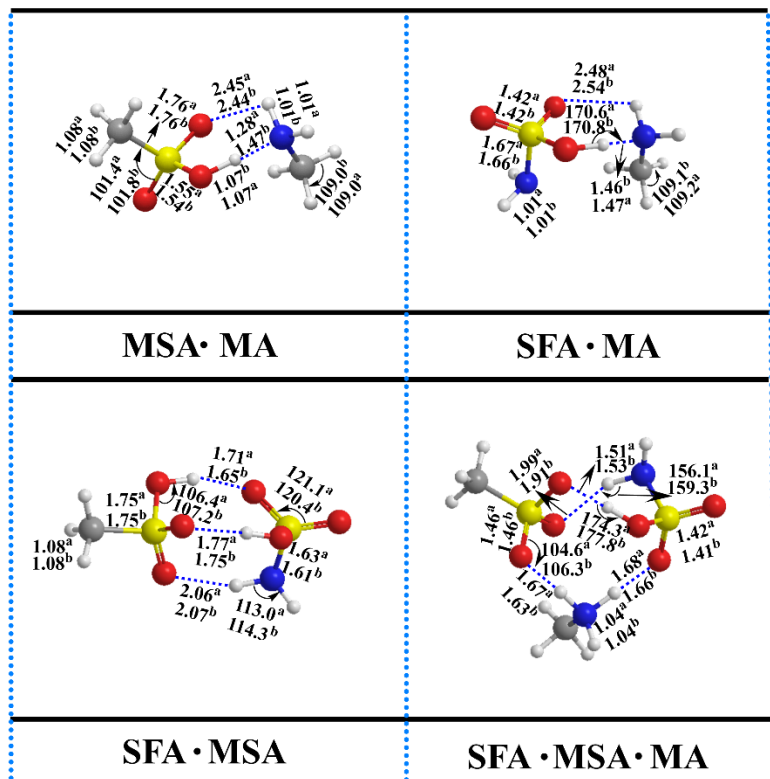
389 **Comment 3.**

390 Thermodynamic parameters, obtained from quantum chemical calculations executed at the M06-
391 2X/6-311++G(2df,2pd) level, were used as inputs for the ACDC model. Please further justify for
392 why the M06-2X/6-311++G(2df,2pd) level of theory was employed to obtain the thermodynamic
393 parameters used as inputs for the ACDC model.

394 **Response:** Thanks for your valuable comments. Many benchmark studies (*Atmos. Chem. Phys.*,
395 2024, 24, 3593-3612; *Atmos. Chem. Phys.*, 2021, 21, 6221-6230; *Atmos. Chem. Phys.*, 2022, 22,
396 1951-1963; *Sci. Total Environ.*, 2020, 723, 137987) show that the M06-2X functional has good
397 performance compared to other common functionals for gaining the Gibbs free energies. For all the
398 M06-2X calculations with the 6-311++G(2df,2pd) basis set was used, as it is a good compromise
399 between accuracy and efficiency and does not yield significant errors in the thermal contribution to
400 the free energy compared to much larger basis sets such as 6-311++G(3df,2pd). So, according to the
401 reviewer’s suggestion, the sentence of “Notably, many benchmark studies (Zhao et al., 2020; Zhang
402 et al., 2024; Tsona Tchinda et al., 2022; Liu et al., 2020) show that the M06-2X functional has good

403 performance compared to other common functionals for gaining the Gibbs free energies. For all the
404 M06-2X calculations with the 6-311++G(2df,2pd) basis set was used, as it is a good compromise
405 between accuracy and efficiency and does not yield significant errors in the thermal contribution to
406 the free energy compared to much larger basis sets such as 6-311++G(3df,3pd), with the differences
407 of relative ΔG less than 1.75 kcal·mol⁻¹ (Table S7).” was added in Line 177 Page 6 to line 183 Page
408 7 of the revised manuscript. Besides, for the optimized geometries of the important precursors of
409 atmospheric aerosol nucleation (MSA, MA and SFA), the main bond lengths and bond angles at
410 two different theoretical levels of M06-2X/6-311++G(2df,2pd) and M06-2X/6-311++G(3df,3pd)
411 has been listed in Fig. S17. Moreover, in Table S7, the predicted relative ΔG of MSA·MA,
412 SFA·MA, MSA·SFA and MSA·SFA·MA clusters at the M06-2X/6-311++G(2df,2pd) level was
413 compared with the corresponding values at the M06-2X/6-311++G(3df,3pd) level. Based on the
414 above analysis, the corresponding changes are as follows.

415 (a) For the MSA·A, SFA·A, MSA·SFA and MSA·SFA·MA clusters, the geometric parameters
416 (Fig. S15) at the M06-2X/6-311++G(3df,3pd) and M06-2X/6-311++G(2df,2pd) levels of theory
417 were calculated. The geometrical structure analysis indicated that the bond lengths and angles
418 obtained from both theoretical levels are close to each other. So, all optimizations and vibrational
419 frequency were calculated at M06-2X/6-311++G(2df,2pd) level.



420

421 **Fig. S17** The optimized geometries of the important precursors of atmospheric aerosol nucleation (MSA, MA and
 422 SFA), especially the main bond lengths and bond angles at two different theoretical levels. SFA, MSA and MA are
 423 the shorthand for formic acid, sulfuric acid and ammonia, respectively. ^a The values obtained at the M06-2X/6-
 424 311++G(2df,2pd) level of theory. ^b The values obtained at the M06-2X/6-311++G(3df,3pd) level of theory. Bond
 425 length is in angstrom and angle is in degree

426 (b) We calculated the Gibbs free energy (in Table S7) for the MSA·MA, SFA·MA, MSA·SFA
 427 and MSA·SFA·MA clusters at the M06-2X/6-311++G(3df,3pd) and M06-2X/6-311++G(2df,2pd)
 428 levels of theory. The analysis of Gibbs free energy indicated that the predicted relative ΔG of
 429 MSA·MA, SFA·MA, MSA·SFA and MSA·SFA·MA clusters at the M06-2X/6-311++G(2df,2pd)
 430 level is nearly close to the values at the M06-2X/6-311++G(3df,3pd) level, with differences of less
 431 than 1.75 kcal·mol⁻¹. So, we chose the M06-2X/6-311++G(2df,2pd) method for further frequency
 432 calculations. Relevant details are presented in Table S7.

433 **Table S7** Comparison of calculated formation free energies (ΔG) at the M06-2X/6-311++G(2df,2pd)
 434 and the M06-2X/6-311++G(3df,3pd) levels

Cluster	M06-2X/6-311++G(2df,2pd)	M06-2X/6-311++G(3df,3pd)
	kcal·mol ⁻¹	
MSA·MA	-6.19	-6.55
MSA·SFA	-9.33	-9.54
MA·SFA	-6.01	-6.98

MSA·MA·SFA	-21.96	-23.71
	(c) In line 177 Page 6 to line 181 Page 7 of the revised manuscript, the reason for selecting the M06-2X/6-311++G(2df,2pd) method has been added and organized as “For all the M06-2X calculations with the 6-311++G(2df,2pd) basis set was used, as it is a good compromise between accuracy and efficiency and does not yield significant errors in the thermal contribution to the free energy compared to much larger basis sets such as 6-311++G(3df,3pd), with the differences of relative ΔG less than 1.75 kcal·mol ⁻¹ (Table S7).”.	

441 **Comment 4.**

442 Page 13 lines 362-366: “Secondly, the contribution of the pathway with SFA exhibits a negative
 443 correlation with [SA] (Fig. 8 (c)), attributed to the competitive relationship between SFA and MSA.
 444 Thirdly, the contribution of the SFA-involved cluster formation pathway was positively associated
 445 with the concentration of [SFA] (Fig. 8 (d))”. Rather than fixing the concentrations of other
 446 precursors and discussing the impact of changes in a single component's concentration, I think it
 447 would be more valuable to explore the specific nucleation mechanisms in regions such as India or
 448 China by incorporating observational concentrations of SFA, MSA, and MA as reported in field
 449 studies.

450 **Response:** Thanks for the suggestion of the reviewer. According to the reviewer's suggestion,
 451 Fig. 8(c) was redrawn to include the branching ratios of the SFA-MSA-MA (pink pie). Besides, in
 452 Lines 395-412 Page 14 of the revised manuscript, the discussion for the branching ratios of the SFA-
 453 MSA-MA has been reorganized. The main changes are as follows.

454 (a) To include the branching ratios of the SFA-MSA-MA, the newly revised Fig. 8(c) was
 455 redrawn and was shown in Revised Manuscript.

456 (b) In Lines 395-412 Page 14 of the revised manuscript, the contribution of SFA to MSA-MA
 457 system influenced by [SFA] and [MSA] has been added and reorganized as “Secondly, as depicted
 458 in Fig. 8(c) and Fig. S22, the contribution of SFA to the MSA-MA system is primarily influenced
 459 by [SFA] and [MSA], with negligible dependence on [MA]. To assess the role of SFA in MSA-MA
 460 nucleation in the atmosphere, the specific contribution of the MSA-MA cluster growth paths at
 461 varying [SFA] to NPF was calculated at 278.15 K, as illustrated in Fig. 8(c), under the ambient

462 conditions typical of the corresponding regions. Generally, as [SFA] increases from 10^4 to 10^8
463 molecules \cdot cm $^{-3}$, the contribution of the SFA-involved pathway increases gradually. Specifically, at
464 low [SFA] (10^4 molecules \cdot cm $^{-3}$), the contributions of SFA-involved clustering pathways are 77%
465 and 41% in regions with relatively low [MSA] in non-sea regions (Berresheim et al., 2002). In
466 regions with high [SFA] (10^6 , 10^8 molecules \cdot cm $^{-3}$), the contributions of the SFA-MSA-MA growth
467 pathways are dominant in their NPF. Particularly in areas with high [MSA], such as the Pacific Rim
468 (6.26×10^8 molecules \cdot cm $^{-3}$ (Saltzman et al., 1986)), the central Mediterranean Sea (2.11×10^8
469 molecules \cdot cm $^{-3}$ (Mansour et al., 2020)) and the Amundsen Sea (3.65×10^9 molecules \cdot cm $^{-3}$ (Jung et
470 al., 2020)), nucleation is primarily driven by the SFA-MSA-MA pathway, contributing to
471 approximately 88% of cluster formation. These results suggest that the influence of SFA is more
472 pronounced in regions with relatively high [MSA]. It is important to note that the [SFA] values
473 discussed in this work are estimated from limited observational data based on the reaction between
474 SO₃ and NH₃ in the atmosphere. Accurate determination of atmospheric [SFA] requires extensive
475 field observations to enable more comprehensive research.”.

476 **Comment 5.**

477 The boundary of the ACDC simulation is the smallest clusters that can be stable enough to grow
478 outside of the simulated system. What's the boundary of the present ACDC simulation?

479 **Response.** Thanks for the suggestion of the reviewer. In ACDC simulations, boundary clusters are
480 those allowed to flux out of the simulation box for further growth. Consequently, the smallest
481 clusters outside the simulated system must be sufficiently stable to prevent immediate evaporation
482 back into the system. Considering the formation Gibbs free energy (Table S7) and evaporation rates
483 (Table S9), the clusters containing MSA and MA molecules and an SFA molecule are the most
484 stable and are therefore allowed to grow to larger clusters, thereby contributing to the rate of NPF.
485 Given the above considerations, clusters (MSA)₄ \cdot (MA)₃, (MSA)₄ \cdot (MA)₃ and SFA \cdot (MSA)₃ \cdot (MA)₃
486 are set as the boundary clusters for the ACDC simulation in this study. Based on the analysis above,
487 the corresponding changes are added in Lines 193-198 Page 7 of the revised manuscript, which has
488 been organized as “Considering the formation Gibbs free energy (Table S7) and evaporation
489 rates (Table S9) of all clusters, the clusters containing pure MSA and MA molecules as well as
490 the clusters containing a SFA molecule are mostly more stable and therefore are allowed to

491 form larger clusters and contribute to particle formation rates. In this case, clusters
492 $(MSA)_4 \cdot (MA)_3$, $(MSA)_4 \cdot (MA)_4$ and $SFA \cdot (MSA)_3 \cdot (MA)_3$ are set as the boundary clusters.”.

493 **Comment 6.**

494 Page 3 line 89: “Due to the concentration of SA ..., MSA-driven NPF has attracted growing
495 attention”.

496 Please use either “MSA” or “ CH_3SO_3H ” consistently to represent methanesulfonic acid. The same
497 issue also appears on representation of sulfamic acid.

498 **Response:**

499 Thanks for the suggestion of the reviewer. We apologize for the misunderstanding about
500 methanesulfonic and sulfamic acid. As the suggestion of the reviewer, the name of methanesulfonic
501 and sulfamic acid have been corrected. Specifically, methanesulfonic and sulfamic acid has been
502 labeled as “sulfamic acid (SFA)” and “methanesulfonic acid (MSA)”, respectively, when they are
503 first used. Besides, when they are used again, methanesulfonic and sulfamic acid has been labeled
504 as “SFA” and “MSA”, respectively.

505 **Comment 7.**

506 2 Page 4 line 107-108: “Atmospheric Clusters Dynamic Code (ACDC) models to evaluate the
507 potential effect of SFA on nucleation and NPF.”

508 Please cite the original publications of ACDC models. Additionally, cite some research to
509 demonstrate the reliability of this method.

510 **Response.**

511 Thanks for the suggestion of the reviewer. We apologized for not referencing the original
512 publications of ACDC models. As the suggestion of the reviewer, the original publications of ACDC
513 models and the researches to demonstrate the reliability of this method have been cited. In Lines
514 107-111 Page 4, “Finally, the atmospheric implications and mechanism of SFA in the MSA-MA-
515 dominated NPF process have been evaluated through density functional theory and the Atmospheric
516 Clusters Dynamic Code (ACDC) models to evaluate the potential effect of SFA on nucleation and
517 NPF.” has been added as “Finally, the atmospheric implications and mechanism of SFA in the MSA-
518 MA-dominated NPF process have been evaluated through density functional theory and the

519 Atmospheric Clusters Dynamic Code (ACDC) (McGrath et al., 2012; Hu et al., 2023; Zhao et al.,
520 2020; Zhang et al., 2024; Tsona Tchinda et al., 2022; Liu et al., 2020) models to evaluate the
521 potential effect of SFA on nucleation and NPF.”

522 **Comment 8.**

523 Page 17 line 473-478: Some references include article links, while others do not. Please unify the
524 reference format.

525 **Response:** Thanks for the suggestion of the reviewer. The reference format has been unified and
526 corrected as follows:

527 (a). In Lines 493-495 Page 17, “[Chen, D., Li, D., Wang, C., Luo, Y., Liu, F., and Wang, W.: Atmospheric implications of hydration on the formation of methanesulfonic acid and methylamine clusters: A theoretical study, Chemosphere., 244, 125538-125547, https://doi.org/10.1016/j.chemosphere.2019.125538, 2020.](#)” has been changed as “[Chen, D., Li, D., Wang, C., Luo, Y., Liu, F., and Wang, W.: Atmospheric implications of hydration on the formation of methanesulfonic acid and methylamine clusters: A theoretical study, Chemosphere., 244, 125538-125547, 2020.](#)”.

534 (b). In Lines 496-497 Page 17, “[Chen, H. and Finlayson-Pitts, B. J.: New particle formation from methanesulfonic acid and amines/ammonia as a function of temperature, Environ. Sci. Technol., 51, 243-252, https://doi.org/10.1021/acs.est.6b04173, 2017.](#)” has been changed as “[Chen, H. and Finlayson-Pitts, B. J.: New particle formation from methanesulfonic acid and amines/ammonia as a function of temperature, Environ. Sci. Technol., 51, 243-252, 2017.](#)”.

539 (c). In Lines 516-517 Page 18, “[Elm, J.: Clusteromics II: methanesulfonic acid-base cluster formation, ACS omega., 6, 17035-17044, https://doi.org/10.1021/acsomega.1c02115, 2021.](#)”
540 has been changed as “[Elm, J.: Clusteromics II: methanesulfonic acid-base cluster formation, ACS omega., 6, 17035-17044, 2021.](#)”.

543 (d). In Lines 521-523 Page 18, “[Freeling, F., Scheurer, M., Sandholzer, A., Armbruster, D., Nödler, K., Schulz, M., Ternes, T. A., and Wick, A.: Under the radar – Exceptionally high environmental concentrations of the high production volume chemical sulfamic acid in the urban water cycle, Water Research., 175, 115706, https://doi.org/10.1016/j.watres.2020.115706, 2020.](#)” has been changed as “[Freeling, F., Scheurer, M., Sandholzer, A., Armbruster, D., Nödler, K., Schulz, M., Ternes, T. A., and Wick, A.: Under the radar – Exceptionally high environmental concentrations of the high production volume chemical sulfamic acid in the urban water cycle, Water Research., 175, 115706, 2020.](#)”

548 K., Schulz, M., Ternes, T. A., and Wick, A.: Under the radar – Exceptionally high
549 environmental concentrations of the high production volume chemical sulfamic acid in the
550 urban water cycle, *Water Research.*, 175, 115706, 2020.”.

551 (e). In Lines 551-552 Page 18, “[Hu, Y., Chen, S., Ye, S., Wei, S., Chu, B., Wang, R., Li, H., and Zhang, T.: The role of trifluoroacetic acid in new particle formation from methanesulfonic acid-methylamine, *Atmos. Environ.*, 311, 120001, <https://doi.org/10.1016/j.atmosenv, 2023.>](#)” has
552 been changed as “[Hu, Y., Chen, S., Ye, S., Wei, S., Chu, B., Wang, R., Li, H., and Zhang, T.: The role of trifluoroacetic acid in new particle formation from methanesulfonic acid-methylamine, *Atmos. Environ.*, 311, 120001, 2023.](#)”.

553 (f). In Lines 558-559 Page 19, “[Kendall, R. A., T. H. D., and Harrison, R. J.: Electron affinities of the first-row atoms revisited. Systematic basis sets and wave functions, *J. Chem. Phys.*, 96, 6796-6806, <https://doi.org/10.1063/1.462569, 1992.>](#)” has been changed as “[Kendall, R. A., T. H. D., and Harrison, R. J.: Electron affinities of the first-row atoms revisited. Systematic basis sets and wave functions, *J. Chem. Phys.*, 96, 6796-6806, 1992.](#)”.

554 (g). In Lines 565-566 Page 19, “[McMurry, P. H.: Formation and growth rates of ultrafine atmospheric particles: a review of observations, *J. Aerosol Sci.*, 35, 143-176, <https://doi.org/10.1016/j.jaerosci.2003.10.003, 2004.>](#)” has been changed as “[McMurry, P. H.: Formation and growth rates of ultrafine atmospheric particles: a review of observations, *J. Aerosol Sci.*, 35, 143-176, 2004.](#)”.

555 (h). In Lines 577-578 Page 19, “[J. S., and Zeng, X. C.: Self-Catalytic reaction of SO₃ and NH₃ to produce sulfamic acid and its implication to atmospheric particle formation, *J. Am. Chem. Soc.*, 140, 11020-11028, <https://doi.org/10.1021/jacs.8b04928, 2018.>](#)” has been changed as “[J. S., and Zeng, X. C.: Self-Catalytic reaction of SO₃ and NH₃ to produce sulfamic acid and its implication to atmospheric particle formation, *J. Am. Chem. Soc.*, 140, 11020-11028, 2018.](#)”.

556 (i). In Lines 579-581 Page 19, “[Liu, J., Liu, Y., Yang, J., Zeng, X. C., and He, X.: Directional proton transfer in the reaction of the simplest criegee intermediate with water involving the formation of transient H₃O⁺, *J. Phys. Chem. Lett.*, 12, 3379-3386, <https://doi.org/10.1021/acs.jpclett.1c00448, 2021.>](#)” has been changed as “[Liu, J., Liu, Y., Yang, J., Zeng, X. C., and He, X.: Directional proton transfer in the reaction of the simplest criegee intermediate with water involving the formation of transient H₃O⁺, *J. Phys. Chem. Lett.*, 12,](#)”.

557

558

559

560

561

562

563

564

565

566

567

568

569

570

571

572

573

574

575

576

577

578 3379-3386, 2021.”

579 (j). In Lines 592-593 Page 19, “Lovejoy, E. R. and Hanson, D. R.: Kinetics and products of the
580 reaction $\text{SO}_3 + \text{NH}_3 + \text{N}_2$, *J. Phys. Chem.*, 100, 4459-4465, <https://doi.org/10.1021/jp952404x>,
581 1996.” has been changed as “Lovejoy, E. R. and Hanson, D. R.: Kinetics and products of the
582 reaction $\text{SO}_3 + \text{NH}_3 + \text{N}_2$, *J. Phys. Chem.*, 100, 4459-4465, 1996.”.

583 (k). In Lines 623-625 Page 20, “Shang, D., Tang, L., Fang, X., Wang, L., Yang, S., Wu, Z., Chen,
584 S., Li, X., Zeng, L., Guo, S., and Hu, M.: Variations in source contributions of particle number
585 concentration under long-term emission control in winter of urban Beijing, *Environ. Pollut.*,
586 304, 119072, <https://doi.org/10.1016/j.envpol.2022.119072>, 2022.” has been changed as
587 “Shang, D., Tang, L., Fang, X., Wang, L., Yang, S., Wu, Z., Chen, S., Li, X., Zeng, L., Guo, S.,
588 and Hu, M.: Variations in source contributions of particle number concentration under long-
589 term emission control in winter of urban Beijing, *Environ. Pollut.*, 304, 119072, 2022.”.

590 (l). In Lines 667-668 Page 21, “Zhang, R., Shen, J., Xie, H. B., Chen, J., and Elm, J.: The role of
591 organic acids in new particle formation from methanesulfonic acid and methylamine, *Atmos.*
592 *Chem. Phys.*, 22, 2639-2650, <https://doi.org/10.5194/acp-22-2639-2022>, 2022.” has been
593 changed as “Zhang, R., Shen, J., Xie, H. B., Chen, J., and Elm, J.: The role of organic acids in
594 new particle formation from methanesulfonic acid and methylamine, *Atmos. Chem. Phys.*, 22,
595 2639-2650, 2022.”.

596 (m).In Lines 669-671 Page 21, “Zhang, T., Wen, M., Cao, X., Zhang, Y., Zeng, Z., Guo, X., Zhao,
597 C., Lily, M., and Wang, R.: The hydrolysis of NO_2 dimer in small clusters of sulfuric acid: A
598 potential source of nitrous acid in troposphere, *Atmos. Environ.*, 243, 117876,
599 <https://doi.org/10.1016/j.atmosenv.2020.117876>, 2020.” has been changed as “Zhang, T., Wen,
600 M., Cao, X., Zhang, Y., Zeng, Z., Guo, X., Zhao, C., Lily, M., and Wang, R.: The hydrolysis of
601 NO_2 dimer in small clusters of sulfuric acid: A potential source of nitrous acid in troposphere,
602 *Atmos. Environ.*, 243, 117876, 2020.”.

603 (n). In Lines 672-674 Page 21, “Zhang, T., Wen, M., Ding, C., Zhang, Y., Ma, X., Wang, Z., Lily,
604 M., Liu, J., and Wang, R.: Multiple evaluations of atmospheric behavior between Criegee
605 intermediates and HCHO: Gas-phase and gas-liquid interface reaction, *J. Environ. Sci.*, 127,
606 308-319, <https://doi.org/10.1016/j.jes.2022.06.004>, 2023.” has been changed as “Zhang, T.,
607 Wen, M., Ding, C., Zhang, Y., Ma, X., Wang, Z., Lily, M., Liu, J., and Wang, R.: Multiple

608 evaluations of atmospheric behavior between Criegee intermediates and HCHO: Gas-phase and
609 gas-liquid interface reaction, *J. Environ. Sci.*, 127, 308-319, 2023.”.

610 (o). In Lines 675-677 Page 21, “[Zhang, T., Wen, M., Zhang, Y., Lan, X., Long, B., Wang, R., Yu, X., Zhao, C., and Wang, W.: Atmospheric chemistry of the self-reaction of HO₂ radicals: stepwise mechanism versus one-step process in the presence of \(H₂O\)_n \(n = 1-3\) clusters, Phys. Chem. Chem. Phys.](#), 21, 24042-24053, <https://doi.org/10.1039/C9CP03530C>, 2019.” has been
611 changed as “[Zhang, T., Wen, M., Zhang, Y., Lan, X., Long, B., Wang, R., Yu, X., Zhao, C., and Wang, W.: Atmospheric chemistry of the self-reaction of HO₂ radicals: stepwise mechanism versus one-step process in the presence of \(H₂O\)_n \(n = 1-3\) clusters, Phys. Chem. Chem. Phys.](#), 21, 24042-24053, 2019.”.

612 (p). In Lines 696-697 Page 21, “[Zhong, J., Kumar, M., Zhu, C. Q., Francisco, J. S., and Zeng, X. C.: Frontispiece: surprising stability of larger criegee intermediates on aqueous interfaces, ANGEW CHEM INT EDIT](#), 56, 7740-7744, <https://doi.org/10.1002/anie.201782761>, 2017.” has been changed as “[Zhong, J., Kumar, M., Zhu, C. Q., Francisco, J. S., and Zeng, X. C.: Frontispiece: surprising stability of larger criegee intermediates on aqueous interfaces, ANGEW CHEM INT EDIT](#), 56, 7740-7744, 2017.”.

613

614

615

616

617

618

619

620

621

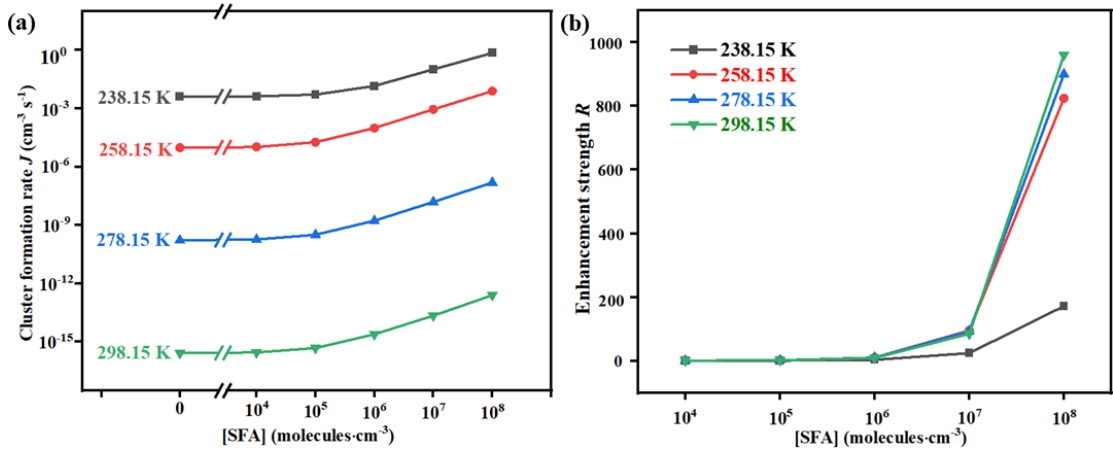
622

623

624 **Comment 9.**

625 The y-axis in Figure 6 contains too much information. It is recommended to adjust the layout to
626 make the results more visually concise.

627 **Response.** Thanks for the suggestion of the reviewer. As the suggestion of the reviewer, the layout
628 in Figure 6 has been adjusted to make the results more visually concise. Specifically, the sentence
629 of “[MSA] = 10⁶, [MA] = 2.5 × 10⁸ (molecules cm⁻³)” have been removed from the Y-axis in Figure
630 6. The newly revised Fig. 6 is shown below.



631

632 **Fig. 6** The J ($\text{cm}^{-3} \text{s}^{-1}$) (a) and R (b) versus $[SFA]$ with $[\text{MSA}] = 10^6$ molecules cm^{-3} , $[\text{MA}] = 2.5 \times$
 633 10^8 molecules cm^{-3} and four different temperatures (green line: 298.15 K, blue line: 278.15 K, red
 634 line: 258.15 K, black line: 238.15 K).

635